Environmental Technology & Innovation 17 (2020) 100580

Contents lists available at ScienceDirect

Environmental Technology & Innovation

journal homepage: www.elsevier.com/locate/eti

Assessment of FlowCam technology as a potential tool for rapid semi-automatic analysis of lacustrine Arcellinida (testate lobose amoebae)

Riley E. Steele [a,*], R. Timothy Patterson [a], Paul B. Hamilton [b], Nawaf A. Nasser [a], Helen M. Roe [c]

[a] Ottawa-Carleton Geoscience Centre and Department of Earth Sciences, Carleton University, 1125 Colonel By Drive, Ottawa, Ontario, K1S 5B6, Canada

[b] Canadian Museum of Nature, Natural Heritage Campus, 1740 Pink Road, Gatineau, Québec, J9J 3N7, Canada

[c] School of Natural and Built Environment, Queen's University Belfast, BT7 1NN, UK

ARTICLE INFO

Article history:
Received 4 October 2019
Received in revised form 13 December 2019
Accepted 13 December 2019
Available online 19 December 2019

Keywords:
Arcellinida
Lake sediments
Micropaleontological analysis
FlowCam VisualSpreadsheet
Flow cytometry
Semi-automated identification

ABSTRACT

This study assessed the possibility of replacing conventional microscopic methods of species-level identification and quantification of Arcellinida with a more rapid method utilizing the FlowCam® with VisualSpreadsheet® (FCVS; Fluid Imaging Technologies, Inc.). Arcellinida are an established group of benthic bioindicators of water and sediment quality in lakes. The use of Arcellinida proxy analysis in lakes and peatlands has dramatically increased since the 1980s, but the labor-intensive nature of identifying and quantifying Arcellinida through microscopy limits the number of samples analyzed. A flow cytometer and microscope with machine learning software has been used to enhance the speed of micropaleontological analysis for some groups (e.g., diatoms), but the potential of using the instrument to analyze Arcellinida in lake sediments has not previously been assessed. The FCVS was assessed here as a method of rapidly analyzing Arcellinida by comparing the results obtained by FCVS with results previously obtained through conventional microscopy in a 2016 study, using the same 46 sediment-water interface samples collected from three quadrats (1–3) in Wightman Cove, Oromocto Lake, New Brunswick, Canada. The FCVS was found to be most suitable for categorizing taxa as morpho-groups rather than using conventional taxonomic species. Therefore, results of the 2016 study were reclassified at the morphological level to facilitate comparison. Results of cluster analysis and Bray–Curtis dissimilarity matrix (BCDM) analysis showed that arcellinidan assemblages obtained through conventional microscopy and FCVS were comparable. Analysis using FCVS reduced operator analysis time by approximately 45%. FCVS shows potential as a reliable method for more rapid analysis of lacustrine Arcellinida, particularly for very large sample data sets; however, FCVS technology can only resolve Arcellinida at the morphological level, meaning that conventional microscopy methods are required if finer species-level taxonomic results are required.

* Correspondence to: School of Geography & Earth Sciences, General Sciences Building, Room 206, McMaster University, 1280 Main Street West, Hamilton, Ontario, L8S 4K1, Canada.
E-mail address: rileysteele@cmail.carleton.ca (R.E. Steele).

https://doi.org/10.1016/j.eti.2019.100580
2352-1864/

1. Introduction

Arcellinida (testate lobose amoebae) are benthic protozoans that are abundant in most freshwater to brackish water sediments (Charman et al., 2000; Patterson and Kumar, 2002). The tests (shells) are preserved in Quaternary lake deposits and can be found throughout the fossil record into the Neoproterozoic (Medioli and Scott, 1983; Medioli et al., 1990a,b; Porter and Knoll, 2000). The beret- or amphora-shaped tests range in size from 30–300 μm. Tests may comprise agglutinated grains from the substrate (xenogenous) or be secreted by the organism (autogenous; Patterson and Kumar, 2002).

During the past few decades, testate amoebae have been analyzed in freshwater habitats across the globe and have been developed into valuable bioindicators of ecosystem health, water quality, seasonal and land-use change (e.g., urbanization, agriculture, forestry, and mining), and paleoenvironments (Creevy et al., 2018; Farooqui et al., 2011; Liu et al., 2019; Marcisz et al., 2019; Nasser et al., 2016; Neville et al., 2010; Patterson et al., 2013; Roe and Patterson, 2006; Roe et al., 2010; Swindles et al., 2018; Taylor et al., 2019). The growing interest in Arcellinida has mainly been linked to their high abundance in organic-rich lake sediments, their rapid reproduction time (days to weeks), the durability of their tests, and their sensitivity to environmental change (Patterson and Kumar, 2002). Compared to other groups of microfossils (e.g., diatoms), Arcellinida within lake samples are taxonomically easy to identify since there are relatively few species in a given sample set (typically only ∼30 species; Supplementary Table 1). However, micropaleontological analysis of each arcellinidan sample still requires several hours (average of nine hours per sample). The most commonly used methods of Arcellinida analysis incorporate labor intensive sample preparation (isolating tests through wet sieving and splitting samples into smaller aliquots) followed by manual identification and quantification of Arcellinida in petri dishes under a microscope (Patterson and Kumar, 2002). For each sample, a statistically significant number of specimens must then be counted. The number of specimens counted per sample depends on the diversity of species observed but is typically ∼150–200 specimens (Patterson and Fishbein, 1989). For an entire sample set, the process can take several weeks to months depending on the total number of samples to be analyzed, so the time required for quantification of specimens in each sample is often the limiting factor with regards to the scale of lacustrine studies undertaken. In order to maximize the potential of Arcellinida as useful and cost effective bioindicators of environmental change in lakes, the development of methods that allow for more rapid identification and enumeration of Arcellinida is desirable.

Recently, instruments that combine flow cytometry, imaging, and particle recognition software have been deployed to rapidly analyze many groups of bioindicators (e.g., diatoms, foraminifera, various algae; (Black et al., 2019; Jyothibabu et al., 2018; Patil and Anil, 2019)), but these methods have not yet been applied to quantitative Arcellinida research. One such instrument, the Flow Cytometer and Microscope (FlowCam®; FC), is equipped with VisualSpreadsheet® (VS) software that is designed to detect, image, enumerate, and characterize microscopic (30–300 μm) particles in a fluid stream (Fluid Imaging Technologies, Inc., 2014; Sieracki et al., 1998)). Here, FCVS technology is assessed as a potential tool for more rapidly detecting, imaging, characterizing, and classifying Arcellinida assemblages within lake sediment-water interface samples. The specific objective of this study is to evaluate the utility of the FCVS in Arcellinida analysis by determining: (1) whether the FCVS-derived arcellinidan assemblages reflect the same environmental variability as observed using conventional microscopy-derived assemblages and; (2) whether or not the instrument can be used to reduce Arcellinida analysis time. If both of these objectives can be met, there is considerable potential for use of the FCVS to permit design and implementation of higher quality, more cost effective, and higher resolution projects.

The FC instrument works by pumping fluid from a sample reservoir through thin plastic tubing into a flow cell composed of a glass chamber where particles are detected and imaged by a camera (Sieracki et al., 1998). The VS software stores the images and characterizes each particle by morphological, gray-scale, color, and spectral measurements. The software allows FCVS operators to create libraries of images that are most representative of target particles. These libraries can then be used to create filters that select for target particles in subsequent sample runs. During post-processing, the filters are used to sort particles that are similar to those in the libraries into separate classes. The more images collected the more refined the libraries become. In this manner, the FCVS can quickly characterize, sort, and count thousands of particles (Fluid Imaging Technologies, Inc., 2014; Sieracki et al., 1998).

Using the FCVS to analyze Arcellinida presents some challenges. The FCVS was originally designed for aqueous applications (Sieracki et al., 1998), although it was subsequently adapted to study particles within sediment samples (D'Anjou et al., 2014; Kitahashi et al., 2018; Magonono et al., 2018; Mani et al., 2019). Sediment-water interface samples, such as those examined for Arcellinida, often contain high amounts of organic and minerogenic matter and generally require additional preparation to prevent blockage of the instrument's flow cell by these particles (Kitahashi et al., 2018). Sample dilution alone is not an efficient option, since this would significantly increase the length of time required for the instrument's sample processing. Conventional organic digestion methods are also not generally suitable as Arcellinida tests are easily damaged (Patterson and Kumar, 2002). Recent research has demonstrated that preparation methods involving chemical deflocculation is most effective for preparing arcellinidan samples for FCVS analysis (Nasser et al., 2019).

Although the FCVS system provides useful particle abundance and size data, it does not reliably provide species-level results (Álvarez et al., 2014; Buskey and Hyatt, 2006; Camoying and Yñiguez, 2016; Kitahashi et al., 2018). Arcellinida generally have a simple morphology and are typically globular, elongate or compressed in shape. Past studies and recent molecular phylogenetic analyses indicate that testate amoebae morphology is closely associated with environmental habitat (Bobrov et al., 1999; Koenig et al., 2018; Lansac-Tôha et al., 2014; Mazei and Warren, 2012; Macumber et al., 2020; Mulot et al., 2017). Therefore, a morpho-group concept of classifying Arcellinida requires further validation and

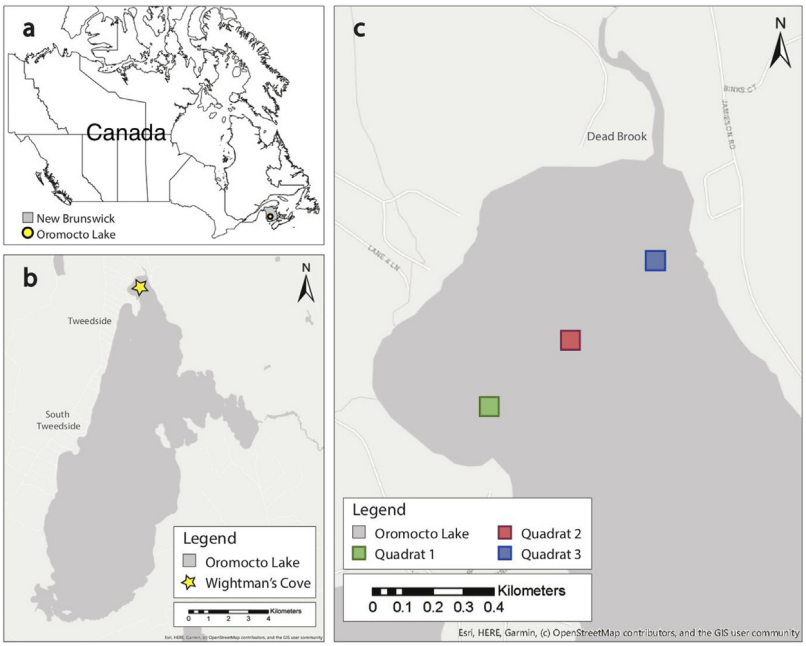

Fig. 1. Map of the study area; **a**. within New Brunswick, Canada; **b**. the location of Wightman Cove, Oromocto Lake, New Brunswick, Canada; and **c**. the sample locations of Quadrats 1, 2, and 3.
Source: Modified from Steele et al. (2018).

is investigated in this study. To this end the FCVS was used to reanalyze samples studied in Steele et al. (2018), recently published research carried out using conventional microscopy.

2. Methods

2.1. Microscope analysis of Arcellinida

2.1.1. Sample collection

Forty-six sediment-water interface samples (upper 3 mm of sediment) were collected from Wightman Cove, Oromocto Lake, Tweedside district, Harvey Station, York County, New Brunswick, Canada on August 3, 2016 (Fig. 1). A detailed description of the study area and field work methods are presented in Steele et al. (2018), which assessed the level of Arcellinida assemblage variability at the species level across a small basin. Samples were collected from three quadrats within Wightman Cove that varied in substrate composition. Quadrat 1 (Q1; 45.641127° (N), −66.999987° (W)) was the shallowest sampling location (3 m) and was characterized by the highest abundance of lake bottom vegetation (∼92% of substrate covered). Quadrat 2 (Q2; 45.641914° (N), −66.997589° (W)) was located in the central part of the basin at a water depth of 5 m, with ∼66% vegetation cover. Quadrat 3 (Q3; 45.642866° (N), −66.994968° (W)) was located in the eastern part of the basin, 300 m south of Dead Brook (a slow-moving inlet stream). Q3 was the deepest sampling location (6 m) and was characterized by an unvegetated muddy substrate (<5% vegetation cover; Fig. 2).

2.1.2. Species-level Arcellinida analysis

Sample preparation, conventional microscopy methods and analytical results obtained through species-level analysis of Wightman Cove samples are reported in Steele et al. (2018). Arcellinida species and informal strains were identified and quantified with reference to well-illustrated papers and keys that follow the same species/strain identification (Kumar and Dalby, 1998; Nasser et al., 2016; Patterson et al., 2012, 2013, 2015; Patterson and Kumar, 2000a,b, 2002; Reinhardt et al., 1998; Roe et al., 2010; Roe and Patterson, 2014).

2.2. FlowCam VisualSpreadsheet® analysis of Arcellinida

2.2.1. Modified sample preparation

Arcellinida-bearing samples typically contain high amounts of sediment and organic matter that can block the flow cell and/or prevent clear images of tests from being captured (Kitahashi et al., 2018). To resolve this issue without damaging tests through harsh digestion methods and without having to increase analysis time through sample dilution, a modified

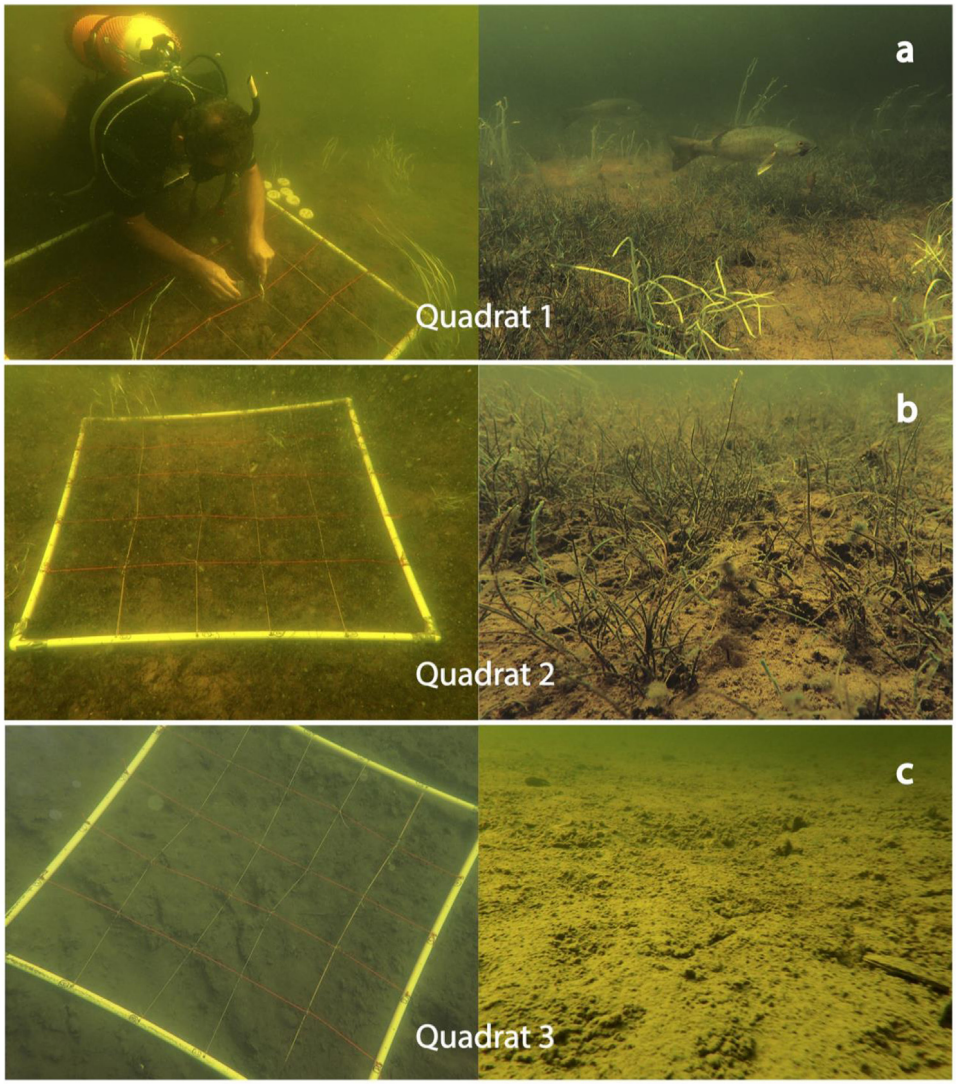

Fig. 2. Photographs of underwater operations during sample collection from three quadrats in Wightman Cove, Oromocto Lake, New Brunswick, Canada; **a**. sampling of Quadrat 1 using SCUBA gear within high aquatic vegetation cover; **b**. more sparsely distributed vegetation in Quadrat 2; and **c**. the muddy, non-vegetated substrate at Quadrat 3. Sixteen samples from each Quadrat were collected, with one sample lost from each of Quadrat 2 and 3 (46 samples total).
Source: Modified from Steele et al. (2018).

sample preparation protocol developed by Nasser et al. (2019) has been implemented in this study. This protocol uses low concentration (5%) potassium hydroxide (KOH), a chemical deflocculant, to disaggregate and remove a portion of organic and minerogenic colloidal matter without severely damaging Arcellinida tests.

Prior to FCVS analysis, six aliquots of each subsample were treated with 5% KOH for one hour. Aliquots were then wet sieved through a 297-μm mesh (for thirty seconds) and a 37-μm mesh (for two minutes) to remove the KOH and any remaining coarse or fine debris. Each aliquot was diluted to 15 ml with distilled water prior to analysis. Even after treatment there was still a relatively high proportion of debris in most samples. Therefore, samples had to be kept in suspension within the sample reservoir, and the high number of debris particles imaged by the instrument increased the overall number of particles to be classified. A combination of chemical treatment and sample dilution limited the number of particles within the flow cell, causing fewer particles to overlap; thus, tests were relatively clearly imaged and identified to the morphological level.

2.2.2. A morpho-group approach

Using extra sediment-water interface samples from the Oromocto Lake sample dataset, several trial runs were completed to determine the FlowCam's image quality and the taxonomic level of Arcellinida that the instrument was able

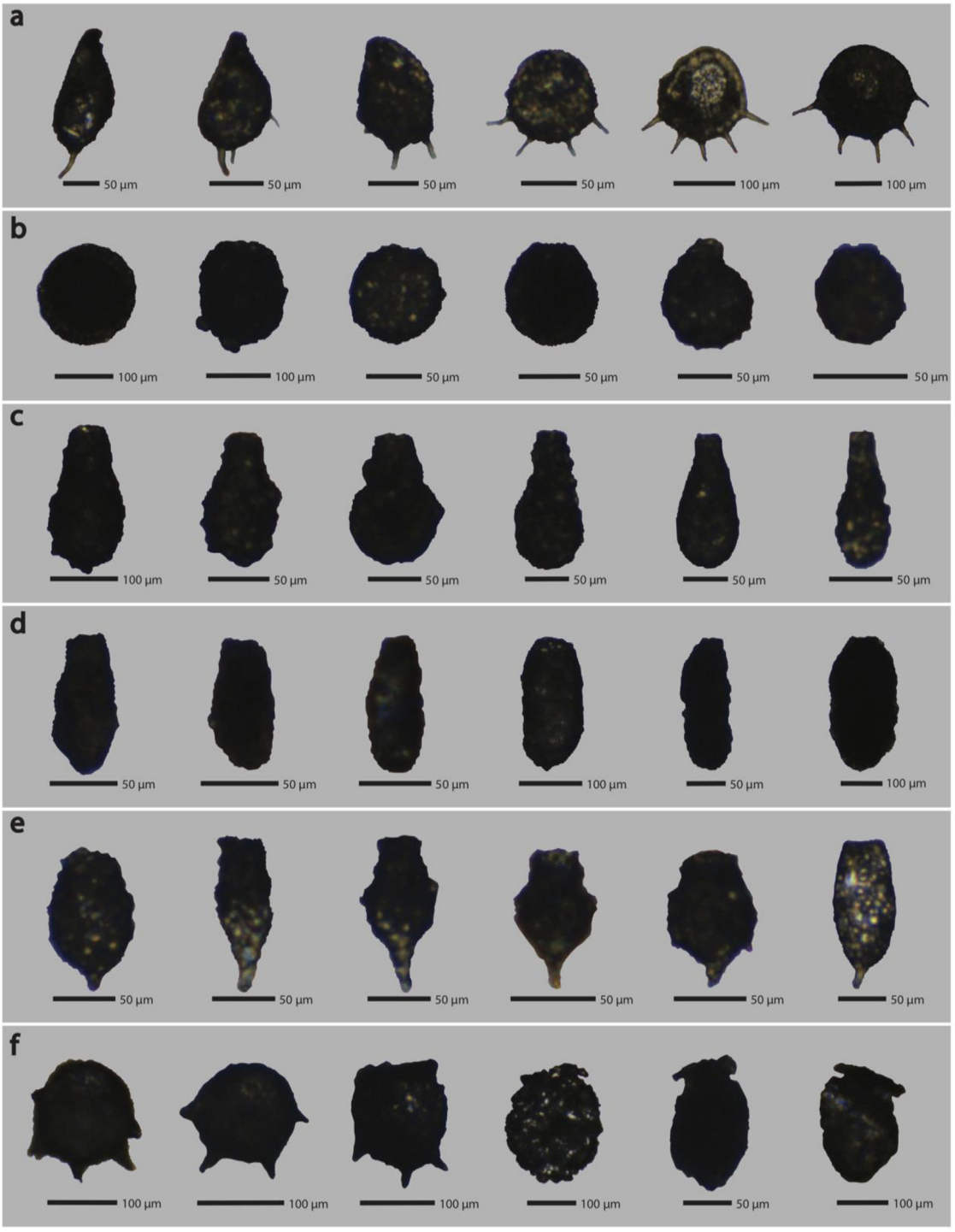

Fig. 3. FlowCam VisualSpreadsheet® derived images of Arcellinida showing the six morpho-groups used for classification: **a**. compressed irregular, **b**. spherical, **c**. pyriform, **d**. linear, **e**. horned, and **f**. collared.

to detect. As a result of the preliminary trials, a classification concept modified from Mazei and Warren's morphological groups of difflugiids (2012, 2014, and 2015) was implemented in this study, which included the following six morpho-groups easily identifiable from the FCVS images (Fig. 3): (1) compressed with irregular shape; (2) spherical or ovoid; (3) pyriform; (4) elongate; (5) horned (aborally spined), and; (6) collared (urceolate, lobed, or teethed). The 28 species

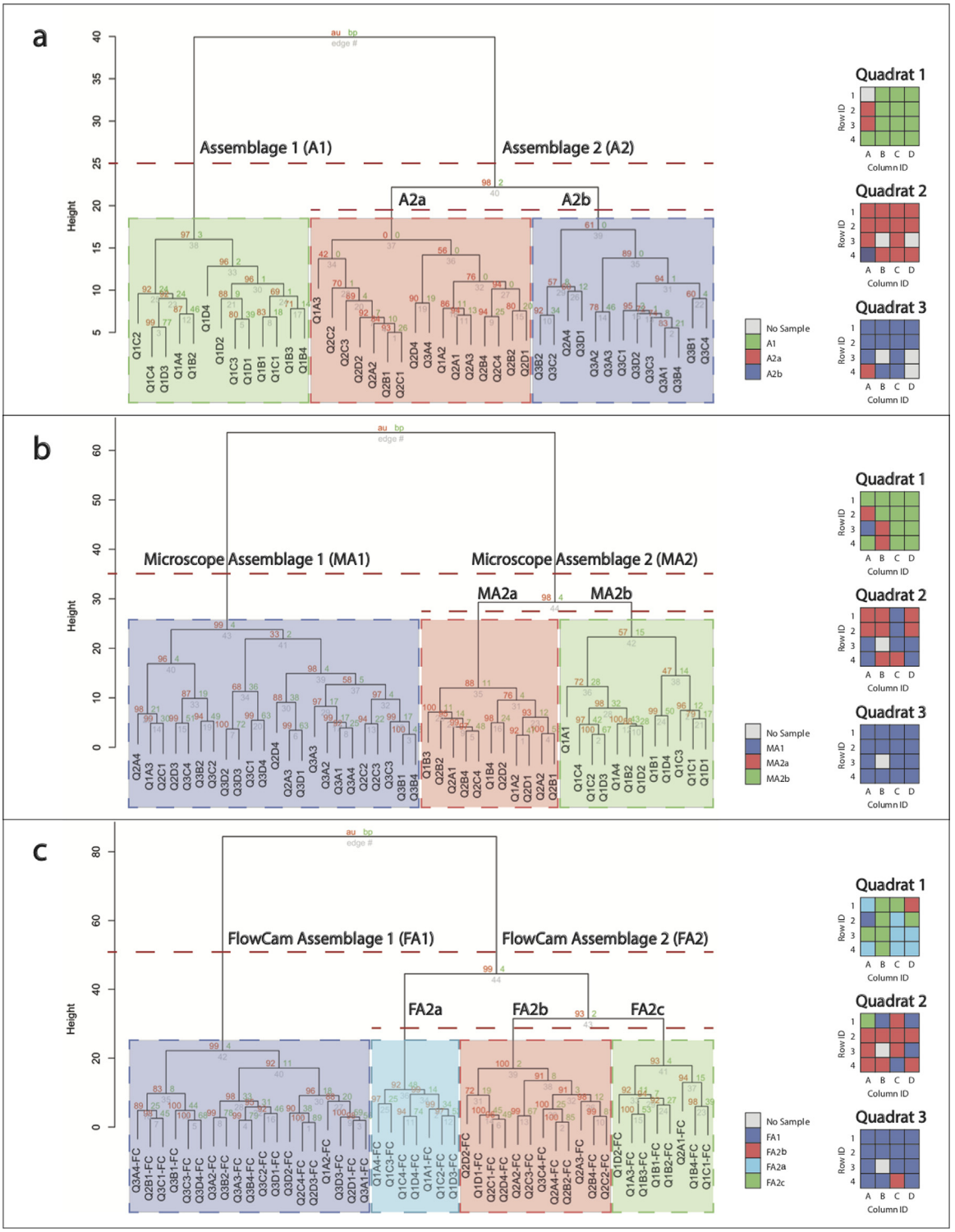

Fig. 4. PVClust cluster analysis dendrogram for the 42 sediment-water interface samples that had no missing values analyzed through **a**. microscopy at the species level in Steele et al. (2018), **b**. microscopy at the morphology level, and **c**. FlowCam at the morphology level. For each analysis, major arcellinidan assemblages and sub-assemblages are indicated as well as assemblage compositions within each Quadrat.

and strains observed in the 46 sediment-water interface samples (Steele et al., 2018) were reclassified into these six morpho-groups, and relative abundances of each morpho-group were tallied (Supplementary Table 2).

Table 1
Median Quadrat Bray–Curtis Dissimilarity Matrix values for morpho-group relative abundances from the:

a. Microscope-obtained dataset			
	Q1 – M	Q2 – M	Q3 – M
Q1 – M	0.0950	0.1313	0.1887
Q2 – M	–	0.0796	0.1177
Q3 – M	–	–	0.0830
b. FlowCam-obtained dataset			
	Q1 – FC	Q2 – FC	Q3 – FC
Q1 – FC	0.1009	0.1557	0.2108
Q2 – FC	–	0.0859	0.1114
Q3 – FC	–	–	0.0652
c. Microscope- and FlowCam- obtained datasets			
	Q1 – FC	Q2 – FC	Q3 – FC
Q1 – M	0.3719	–	–
Q2 – M	–	0.4410	–
Q3 – M	–	–	0.4024

2.2.3. FlowCam sample processing

Arcellinida analysis was carried out on each of the six aliquots of all 46 sediment-water interface samples by the FCVS on Auto Image Mode at 4X magnification with a FC300 (300 μm deep) flow cell. At the beginning of each day of operation, the microscope was manually focused using extra sediment-water interface samples from the dataset. Prior to each sample run, the instrument was flushed and primed with distilled water. Each 15 ml aliquot was processed at a flow rate of 1.7 ml/min and imaged at a constant rate of 20 frames per second (the suggested settings for the particle and sample size used). To minimize blockage to the flow cell, samples were kept in suspension within the sample holder using a stir rod. For most samples, adequately clear images of tests were captured by the FCVS, including at least five target images that could be selected for each library. There was an issue with the FC300 model in that the flow cell is slightly wider than the objective lens. This results in some particles in the fluid flow passing outside the field of view of the digital camera, and as a result these particles, presumably including some Arcellinida specimens, were not imaged. This issue has been addressed in newer FlowCam models where the objective lens is now as wide as the flow cell.

2.2.4. Post-processing with VisualSpreadsheet®

Within the Library window of VS, 49 operator-created libraries were chosen by selecting images that captured most types, sizes, and orientations of particles (including organic and minerogenic debris, pollen, diatoms, and Arcellinida tests). Statistical filters were then generated by the software from the library images, and several operator-defined value filters were created to help ensure accurate sorting of particles. A classification template called 'Arcellinida' was created within the VS Classification Window. The template included 15 classes containing the previously generated statistical and value filters. Six classes containing no filters were added to the template, corresponding to the six morphological groups used in this study.

The aliquots of each of the 46 sediment-water interface samples were processed using the 'Arcellinida' template. When running the "real-time" automated classification, the software was able to perform preliminary sorting, but could not reliably distinguish tests from debris particles. For each aliquot, particles were automatically sorted into the first 15 classes by the software, and any identified tests were manually moved by the operator into one of the six classes corresponding to morphology (Fig. 3). In this manner, Arcellinida tests were identified to a morphological level and quantified until a statistically significant number of tests (>150 per sample) was reached (Patterson and Fishbein, 1989). The FlowCam data was exported into an Excel Spreadsheet, and relative abundances were recorded (Supplementary Table 3).

2.3. Statistical methods

Statistical analyses were carried out on the two microscope datasets and the FlowCam dataset using RStudio (version 1.1.463). Q-mode cluster analysis was performed on the three datasets separately, using Ward's Minimum Variance method (Ward, 1963) to group samples containing similar arcellinidan assemblage compositions (after Fishbein and Patterson, 1993). The PVClust package was used to determine the statistical significance of the identified assemblages (Fig. 4). A Bray–Curtis dissimilarity index matrix (BCDM; Bray and Curtis, 1957) was generated using the two morphology-level datasets to assess the level of similarity between and within the relative abundances obtained through microscopy and through FlowCam (Table 1, Supplementary Table 4).

Table 2
Comparison of microscope and FlowCam VisualSpreadsheet® Arcellinida analysis time per sample.

	Microscope	FlowCam
Subsampling (3 cc)	1 min	1 min
Splitting (into 6 aliquots)	1 h	1 h
Chemical deflocculation	–	1 h
Sieving	2 min	2 min
FlowCam processing 6 aliquots × ∼8 min/aliquot	–	48 min
Test ID/Quantification Microscope: ∼4 aliquots, 120 min/aliquot FlowCam: ∼2 aliquots, 60 min/aliquot	8 h	2 h
Total analysis time per sample	9 h 3 min	4 h 51 min

2.4. Analysis time comparison: Microscope vs FlowCam

To determine whether FCVS analysis was able to reduce Arcellinida analysis time, each step of preparation and analysis using conventional microscopy and FCVS was recorded to generate an estimated average duration time per sample (Table 2). The average times were estimated based on the amount of time it would take an experienced individual to complete each step of Arcellinida analysis on samples containing average sizes and concentrations of tests and debris. The average times excluded consideration for the time required to create the FCVS libraries, filters, and the classification template, since they can all be saved, quickly modified, and reused on future sample sets.

3. Results

3.1. Cluster analysis

3.1.1. Identified Arcellinidan assemblages

The Q-mode PVClust cluster analysis of the 28 Arcellinida species recognized within the 46 sediment-water interface samples (Steele et al., 2018) identified two distinct assemblages: Assemblage 1 (A1; Approximately Unbiased (AU) p-value = 0.97) and Assemblage 2 (A2; AU p-value = 0.98) (Fig. 4a). Within A2, sub-assemblages A2a and A2b were identified at a lower level of significance (AU p-values = 0.00 and 0.61). The identified assemblages and sub-assemblages corresponded well with the three sampling locations including Q1 (A1), Q2 (A2a), and Q3 (A2b), with the exception of four outliers: Q1A2, Q1A3 and Q3A4 clustered with Q2 samples in A2a, and Q2A4 with Q3 samples in A2b (Fig. 4a).

The PVClust cluster analysis results from the morphology-level microscope dataset showed two statistically significant assemblages (Fig. 4b): Microscope Assemblage 1 (AU p-value = 0.99) and Microscope Assemblage 2 (AU p-value = 0.98). MA2 was further divided into two statistically less significant groups recognized as sub-assemblages: MA2a and MA2b (AU p-values = 0.88 and 0.57, respectively). These three groupings roughly correspond to the three sampling locations, with eight outliers clustering with Q3 samples (Q1A3, Q2A4, Q2C1, Q2D3, Q2D4, Q2A3, Q2C2, and Q2C3) and three outliers clustering with Q2 samples (Q1B3, Q1B4, and Q1A2) (Fig. 4b).

The FlowCam dataset grouped into two distinct assemblages at a high statistical significance (AU p-value = 0.99): FlowCam Assemblages 1 and 2 (Fig. 4c). FA2 was further divided into three sub-assemblages: FA2a, FA2b, and FA2c (AU p-values = 0.92, 1.00, and 0.93, respectively). In this case, FA1 corresponded to sampling location Q3, FA2b corresponded with Q2, and samples within FA2a and FA2c corresponded with Q1. There were 8 outliers observed: Q2B1, Q2C4, Q2D3, Q1A2, Q2D1 clustered with Q3 samples; Q1D1 and Q3C4 grouped with Q2 samples; and Q2A1 clustered with Q1 samples (Fig. 4c)".

3.1.2. Faunal structure of assemblages

Within the dataset analyzed by conventional microscopy, the relative abundances of morphologies showed highly similar faunal structure between assemblages associated with Q3 and Q2 samples: MA1 was co-dominated by pyriform (33%) and spherical morphologies (29%), followed by compressed irregular (14%), horned (11%), linear (9%), and collared tests (4%); MA2a had similarly higher proportions of pyriform tests (29%) followed by spherical (24%), compressed irregular (21%), and horned (14%), linear (9%), and collared tests (3%) (Fig. 5a). These relative abundances of morphologies are consistent with the fauna observed in Steele et al. (2018). A2b and A2a, the assemblages associated with Q3 and Q2 samples, were dominated by a pyriform species (*Difflugia oblonga* Ehrenberg, 1832 strain "oblonga" at 26% in A2b and 11% in A2a), and spherical species (12% *Difflugia glans* Penard, 1902 strain "glans", 8% *Lesquereusia spiralis* (Ehrenberg, 1840), and 5% *Cucurbitella tricuspis* (Carter, 1856) in A2b; 11% *D. glans* "glans", and 7% *L. spiralis* in A2a). In both assemblages, a horned species, *Difflugia elegans* Penard, 1890, was observed at relatively high frequency (7%) (Steele et al., 2018).

The microscope-obtained morphological assemblage that corresponded to Q1 samples was composed of more evenly distributed morphologies: MA2b was co-dominated by compressed irregular (23%), pyriform (22%), and spherical tests

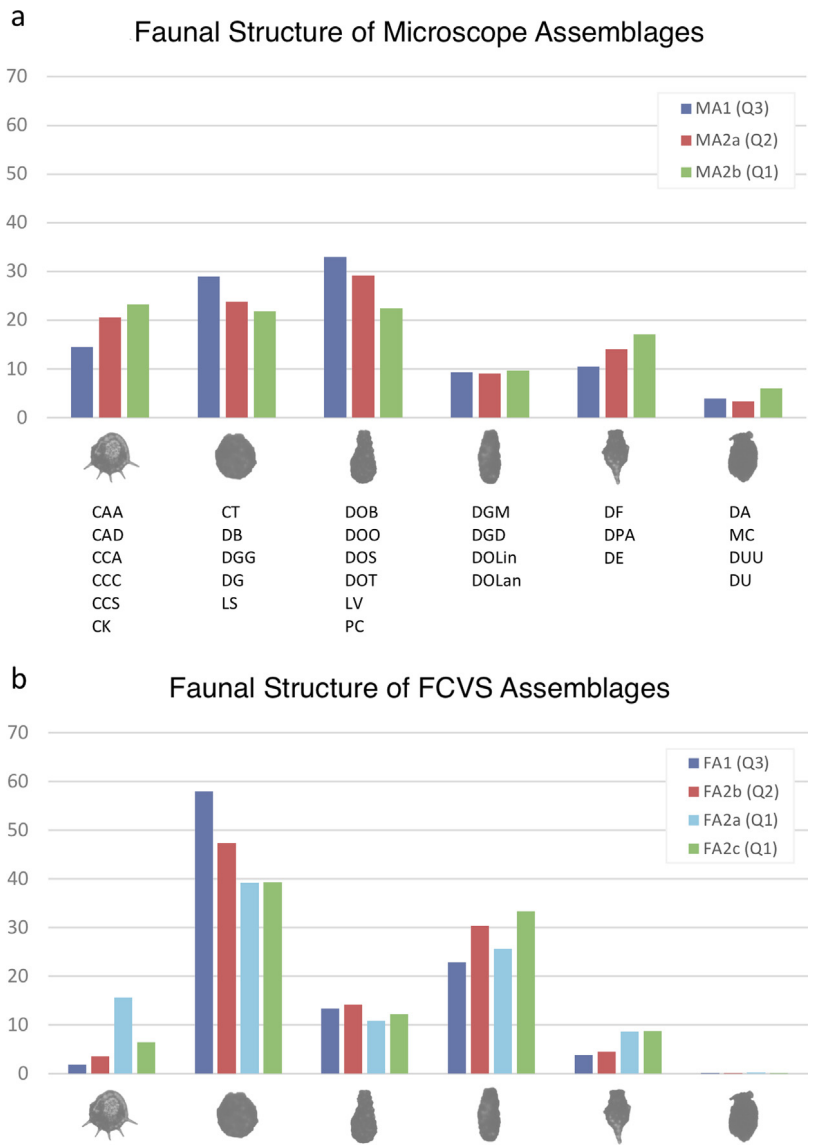

Fig. 5. Relative abundances of morpho-groups in **a**. the microscope-derived assemblages, and **b**. the FlowCam-derived assemblages. Species included in each morphological class are shown in a. CCA *Centropyxis aculeata* "aculeata", CAD *C.a.* "discoides", CCA *C. constricta* "aerophila", CCC *C.c.* "constricta", CCS *C.c.* "spinosa", CK *Cyclopyxis khali*, CT *Cucurbitella tricuspis*, DB *Difflugia bidens*, DGG *D, glans* "glans", DG *D. globulosa*, LS *Lesquereusia spiralis*, DOB *D. oblonga* "bryophila", DOO *D.o.* "oblonga", DOS *D.o.* "spinosa, DOT *D.o.* "tenuis", LV *Lagenodifflugia vas*, PC *Pontigulasia compressa*, DGM *D. glans* "magna", DGD *D. glans* "distenda", DOLin *D.o.* "linearis", DOLan *D.o.* "lanceolata", DF *D. fragosa*, DPA *D. protaeiformis* "acuminata", DE *D. elegans*, DA *D. amphora*, MC *Mediolis corona*, DUU *D. urceolata* "urceolata", DU *D. urens*.

(22%), followed by horned (17%), linear (10%), and collared (6%) tests (Fig. 5a). This relative increase in compressed irregular species and decrease in pyriform species compared to MA1 and MA2a was consistent with the fauna observed in Steele et al. (2018). A1, the assemblage associated with Q1 samples, was dominated by *D. oblonga* "oblonga" (19%), *D. elegans* (11%), two compressed irregular strains (9% *Centropyxis aculeata* (Ehrenberg, 1832) strain "aculeata" and 6% *Centropyxis constricta* (Ehrenberg, 1843) strain "aerophila"), and 7% *D. glans* "glans" (Steele et al., 2018).

All four FCVS-obtained assemblages were similar in their faunal structure. FA1, corresponding with Q3 samples, was dominated by spherical tests (58%), followed by linear (23%), pyriform (13%), horned (4%), compressed irregular (2%), and collared (<1%); FA2b (associated with Q2 samples) had similarly higher proportions of spherical (47%) and linear tests (30%), with lower abundances of pyriform (14%), horned (5%), compressed irregular (4%), and collared tests (<1%) (Fig. 5b). The two assemblages found within Q1 samples were highly comparable, with the main difference being the abundance of compressed irregular tests: FA2a was dominated by spherical morphologies (39%), followed by linear (26%), compressed irregular (16%), pyriform (11%), horned (8%), and collared tests (<1%); and FA2c had higher abundances of

spherical (39%), linear (33%), and pyriform tests (12%), with lower proportions of horned (9%), compressed irregular (6%), and collared (<1%) tests (Fig. 5b).

The faunal assemblage structures identified using conventional microscopy and FCVS were notably different. A higher proportion of pyriform tests were identified through conventional microscopy, while spherical and linear tests were more frequently identified using FCVS. The identification of collared tests (urceolate, lobed, or teethed) using FCVS images was significantly reduced compared to the proportions identified using conventional microscopy (Fig. 5).

3.2. Bray–Curtis dissimilarity matrix

The results of the BCDM show statistically measurable similarities within the conventional microscopy dataset and the FCVS dataset. The results of this analysis also show the statistically measured differences in morpho-group relative abundances between the two methods (Table 1, Supplementary Table 3). Differences between sampling locations were also measured within each method. The BCDM dissimilarity coefficients range from 0–1 and can be perceived as a percentage of similarity. For instance, within the conventional microscopy dataset (Table 1a) a comparison within Q1 samples resulted in a mean dissimilarity coefficient of 0.0950. This indicates that the relative abundances of morpho-groups within Q1 samples were approximately 90.5% similar. In the same manner, Q2 samples were approximately 92.0% similar to each other, and Q3 samples were approximately 91.7% similar. The samples from Q1 were more similar to those from Q2 (86.9%) than samples from Q3 (81.1%), and samples from Q2 were relatively similar to those from Q3 (88.2%) (Table 1a). This higher similarity between Q1 and Q2 samples, as well as between Q2 and Q3 samples, support the slight overlaps with these quadrats observed in the cluster analysis (Fig. 4b).

Within the FCVS dataset (Table 1b), the relative abundances in samples within each quadrat were highly similar (89.9% similarity within Q1, 91.4% similarity within Q2, and 93.5% similarity within Q3 samples). The BCDM results showed a lower similarity between Q1 and Q3 samples (78.9%) than between Q1 and Q2 samples (84.4%) or Q2 and Q3 (88.9%) (Table 1b). These observations are consistent with the results of conventional microscopy cluster analysis, which found the greatest difference between Q1 and Q3 samples (Fig. 4c). Although Q1 clustered into two sub-assemblages (FA2a and FA2c; Fig. 4c), the BCDM indicated that relative abundances in Q1 samples were highly similar, suggesting that FA2a and FA2c could be considered a single sub-assemblage.

When comparing the relative abundances obtained from conventional microscopy and the FCVS method (Table 1c), the differences between Q1 samples were notable (only 62.8% similar) and the differences between Q2 and Q3 were both quite significant (similarities of 55.9% and 59.8%, respectively). These results further describe the differences observed between the two methods when comparing the faunal assemblage makeup.

3.3. Analysis time comparison: Microscope vs FlowCam

Arcellinida analysis times required using conventional microscopy and the FCVS were compared (Table 2). It was estimated that sample preparation for microscopy (including subsampling, wet splitting, and sieving methods) took approximately 1 h and 3 min per sample, while sample preparation for the FCVS took an additional hour for chemical deflocculation (2 h and 3 min total). The FCVS protocol required approximately 48 min to process each sample, including all 6 aliquots at an average run time of 8 min per aliquot. In order to identify and quantify >150 tests per sample, an average of 4 aliquots was required to be analyzed for microscopy and 2 aliquots using FCVS. This process was estimated to take 8 h per sample (120 min per aliquot) for microscopy and 2 h per sample (60 min per aliquot) for post-processing FCVS data. In total, it would take an estimated 9 h and 3 min for conventional microscopic Arcellinida analysis of a single sample, and 4 h and 51 min for FCVS analysis (Table 2).

4. Discussion

4.1. Method modifications

One of the major challenges to FCVS analysis of lacustrine Arcellinida is the organic-rich nature of the sediment-water interface samples. Running samples that have been processed using standard preparation methods (sieving and splitting only) is not possible due to sediment build-up within the narrow FC tubing. Kitahashi et al. (2018) also acknowledged this difficulty with the instrument when running marine sediment samples. To solve this problem, they used a high-density solution instead of water. Here, this issue was mitigated by treating samples with a chemical deflocculant, 5% KOH. Removing a portion of organic and minerogenic colloidal matter considerably reduced the frequency of sediment build-up and reduced the amount of debris particles imaged. The treatment did not seem to cause severe damage to Arcellinida tests, as there were no observable differences in the number of broken tests compared to the previous microscopic analysis (estimated <5% of broken tests in both cases). The additional sample preparation protocols employed in this study using the recommended approach of Nasser et al. (2019) greatly improved the utility of the FCVS for processing organic-rich sediment samples.

The FCVS low image resolution and limited ability to resolve taxonomic units lower than genus level has been acknowledged in several recent studies (Álvarez et al., 2014; Buskey and Hyatt, 2006; Camoying and Yñiguez, 2016;

Kitahashi et al., 2018). Some FlowCam users have attempted to optimize the FCVS hardware and software settings to obtain higher resolution images (Camoying and Yñiguez, 2016), while other researchers suggest re-examining samples under a microscope when encountering specimens that are difficult to identify from FCVS images (Buskey and Hyatt, 2006; Kitahashi et al., 2018). Alternatively, it has been found that classifying FCVS imaged taxa into "functional classes" of higher taxonomic groupings or "shape classes" based on morphology is often sufficient for most ecological studies (Álvarez et al., 2014).

The species-level microscopy results from Steele et al. (2018) clustered into three assemblages (A1, A2a, and A2b), which reflected the three different ecological environments within Wightman Cove, Oromocto Lake. In that previous study, the high diversity of A1 corresponded with the shallow, densely vegetated location of Q1; the lower diversity of A2b was related to the deeper, non-vegetated site of Q3 and its close proximity to runoff from Dead Brook. A2a was characteristically similar to A1 and A2b, reflecting the mid-basin environment of Q2 between Q1 and Q3 (Figs. 2 and 4a; Steele et al., 2018). When reclassifying the microscope-obtained data into six major morpho-groups, statistical analyses recognized the same distinct variation in assemblages between samples from Q1 and Q3, and a significant similarity of Q2 samples with the assemblages from Q1 and Q3 (Fig. 4b, Table 1). These results suggest that the species level arcellinidan assemblages resulting from slight substrate differences between the three sampling locations were also observed at the morphological level. This indicates that the morphology-level conventional microscope dataset was reliable and could be used as an alternative taxonomic database for evaluation of the FCVS-obtained results as found by Álvarez et al. (2014).

4.2. FlowCam Arcellinidan assemblage variability

The PVClust cluster analysis results of the FCVS-obtained dataset showed that Q1 was characterized by two distinct sub-assemblages (FA2a and FA2c; Fig. 4c). This slight division between Q1 samples can be observed in the faunal structures where FA2a contains a higher abundance of compressed irregular tests than FA2c (16% and 6%, respectively). The low mean dissimilarity coefficient (0.1009) derived from the BCDM, however, indicated that the two sub-clusters could be considered one sub-assemblage (Table 1).

Other than the division within Q1 samples, the cluster results from the FCVS dataset were nearly identical to those obtained through microscopy. Although the assemblages identified using both methods corresponded well to sample location, the faunal structures discriminated using the two methods differed considerably (Fig. 5). When comparing the relative abundances between the two methods, the BCDM resulted in a similarity of only 55.9–62.8%.

The FCVS method more frequently identified spherical and linear morphologies compared to conventional microscopy; and although collared tests were rarely counted during microscopy (3%–6%), their identification was extremely rare during FCVS analysis (<1%). This considerable difference in relative abundances of morpho-groups between the two methods could be attributed to image resolution and specimen orientation with the FCVS. Morphologies that have smoother textures (e.g., spherical and linear) may be more distinguishable from debris particles and therefore more easily recorded from FCVS images. Many Arcellinida, especially Centropyxids and those within the collared morpho-group, have distinguishing characteristics that can be hidden by certain orientations. Since FCVS does not allow for manual manipulation of tests orientation (as in conventional microscopy), this could explain why certain groups were recorded less frequently during FCVS analysis. The assemblage results from both methods should still be valid, since in both cases a statistically significant number of tests were counted.

The overall comparison of Arcellinida analysis results suggest that both conventional microscopy and the FCVS methods distinguish the same variation in morphological assemblages. It is likely that these assemblage patterns are both a result of slight differences in sampling environment; therefore, the results support the use of FCVS as an effective tool for analyzing Arcellinida at the morphological level.

4.3. FlowCam VisualSpreadsheet® Arcellinida analysis time

In addition to testing whether or not variations in Arcellinida assemblages could be accurately detected from FCVS-obtained data, it was important to know whether the instrument was able to reduce analytical time. After comparing the time it would take an experienced operator to perform each step of Arcellinida analysis (including sample preparation and the identification and quantification of specimens) using either conventional microscopy or the FCVS, it was determined that, despite having to carry out sample deflocculation, the FCVS was able to reduce analysis time by roughly 45% (Table 2). This represents a significant time saving, particularly for projects where there are a large number of samples.

There can be a significant difference between sediment samples with regard to the organic and minerogenic content, as well as the total concentration and size of contained Arcellinida specimens. These factors can affect overall analysis time, though both conventional microscopic and FCVS methods would be equally affected. It is also possible that identification and quantification times required for Arcellinida analysis using conventional microscopic approaches might be reduced if disaggregation methods were applied during standard sample preparation (Nasser et al., 2019). However, it is likely that the FCVS approach would still significantly reduce required overall analytical time.

5. Summary and conclusions

This study was designed to assess the possibility of replacing conventional microscopic methods of species-level identification and quantification of Arcellinida with a more rapid FCVS-based method. The dataset employed was comprised of 46 samples from three quadrats (stations) in Wightman Cove, Oromocto Lake, New Brunswick, Canada, which had previously been analyzed using conventional microscopy (Steele et al., 2018). It was determined that FCVS could provide a 45% saving in analytical time despite having to employ an additional preparation technique whereby samples had to be left for one hour in a 5% KOH solution to deflocculate organic debris, which tends to clog the flow cell in the FCVS. The FCVS was inferior to conventional microscopy in that the lower resolution microscope in the instrument made it difficult for it to resolve specimens to the species or strain level. However, when a morpho-group approach to taxonomic division was employed, for both FCVS and conventional microscopy, very similar results were obtained. The six morphological groups used in this study, based on Mazei and Warren (2012, 2014, 2015) morphological groupings of difflugiids were easily identified from the imaged particles (Fig. 3). Since the assemblages obtained through FCVS were comparable to morpho-groups distinguished through microscopy, the results reported here support the use of a morphological classification scheme for Arcellinida research.

Although the software could not automatically distinguish between tests and debris particles, the software's classification resulted in categories of characteristically similar particle images for more efficient manual identification and enumeration of tests. In addition to poor image (and therefore taxonomic) resolution and the software's inability to 'identify' specific Arcellinida taxa, another limitation of the instrument and software was the learning curve associated with becoming proficient with the instrument (e.g., determining optimal instrument settings and input parameters for the creation of libraries, filters, and classification templates, etc.). Another drawback was specimen loss during analysis. With the FC300 model used here, some specimens in the fluid flow were outside the field of view of the objective lens, meaning it was difficult to ensure imaging of all specimens in a sample. Furthermore, any remarkable specimens observed during FCVS analysis cannot be easily retrieved by the user for more detailed examination.

Arcellinida analysis using the FCVS was only possible when carried out semi-manually at the morphological level, but the FCVS-obtained assemblages did reflect substrate variation in the same manner as the conventional microscopy-obtained results (Fig. 4). It was determined that the FlowCam can reduce Arcellinida analysis time by a significant amount (Table 2), once the learning curve associated with the instrument and software is overcome. This study indicates that the FCVS has potential as a method for more rapid analysis of Arcellinida but cannot fully replace conventional microscopic methods where identification of specific taxa is required. The FCVS is potentially a more useful method for analyzing large numbers of samples but will provide coarser taxonomic resolution assemblage results. The more labor- and time-intensive microscopic methods may be a better option for analyzing smaller data sets and will provide species-level assemblage results.

Declaration of competing interest

The authors declare that they have no known competing financial interests or personal relationships that could have appeared to influence the work reported in this paper.

CRediT authorship contribution statement

Riley E. Steele: Methodology, Investigation, Formal analysis, Visualization, Writing - original draft, Writing - review & editing, Data curation. **R. Timothy Patterson:** Conceptualization, Project administration, Funding acquisition, Resources, Supervision, Writing - review & editing. **Paul B. Hamilton:** Project administration, Funding acquisition, Resources, Supervision, Writing - review & editing. **Nawaf A. Nasser:** Methodology, Formal analysis, Software, Visualization. **Helen M. Roe:** Writing - review & editing.

Acknowledgments

We thank Roy and Jean Patterson for their logistical support during fieldwork, and Malcolm Patterson for assistance with underwater photography. We also thank those at the Canadian Museum of Nature's Natural Heritage Campus for the use of their FlowCam® system.

Funding

This research was funded by NSERC Discovery (Canada) and Carleton University Development (Canada) grants awarded to R. Timothy Patterson.

Appendix A. Supplementary data

Supplementary material related to this article can be found online at https://doi.org/10.1016/j.eti.2019.100580.

References

Álvarez, E., Moyano, M., López-Urrutia, A., Nogueira, E., Scharek, R., 2014. Routine determination of plankton community composition and size structure: a comparison between FlowCAM and light microscopy. J. Plankton. Res. 36 (1), 170–184.

Black, J.G., Stark, J.S., Johnstone, G.J., McMinn, A., Boyd, P., McKinlay, J., Wootherspoon, S., Runcie, J.W., 2019. In-situ behavioural and physiological responses of Antarctic microphytobenthos to ocean acidification. Sci. Rep. 9, 1890–1903.

Bobrov, A.A., Charman, D.J., Warner, B.G., 1999. Ecology of testate amoebae (Protozoa: Rhizopoda) on peatlands in western Russia with special attention to niche separation in closely related taxa. Protist 150 (2), 125–136.

Bray, J.R., Curtis, J.T., 1957. An ordination of the upland forest communities of southern Wisconsin. Ecol. Monogr. 27, 325–349.

Buskey, E.J., Hyatt, C.J., 2006. Use of the FlowCAM for semi-automated recognition and enumeration of red tide cells (*Karenia brevis*) in natural plankton samples. Harmful Algae 5, 685–692.

Camoying, M.G., Yñiguez, A.T., 2016. FlowCAM optimization: Attaining good quality images for higher taxonomic classification resolution of natural phytoplankton samples. Limnol. Oceanogr. Methods 14, 305–314.

Carter, H.J., 1856. Notes on the freshwater Infusoria of the island of Bombay. Ann. Mag. Nat. Hist. 18 (104), 115–132.

Charman, D.J., Hendon, D., Woodland, W., 2000. The identification of peatland testate amoebae. Quaternary Research Association Technical guide no. 9 London, 147 pp.

Creevy, A.L., Andersen, R., Rowson, J.G., Payne, R.J., 2018. Testate amoebae as functionally significant bioindicators in forest-to-bog restoration. Ecol. Indic. 84, 274–282.

D'Anjou, R.M., Balascio, N.L., Bradley, R.S., 2014. Locating cryptotephra in lake sediments using fluid imaging technology. J. Paleolimnol. 52, 257–264.

Ehrenberg, C.G., 1832. Über die Entwicklung und Lebensdauer der Infusionsthiere, nebst ferneren Beiträgen zu einer Vergleichung ihrer organischen Systeme. Abh. Dtsch. Akad. Wiss. Berl., Kl. Math. 1831, 1–154.

Ehrenberg, C.G., 1840. Das grössere Infusorienwerk. Abh. Dtsch. Akad. Wiss. Berl., Kl. Math. 19, 8–219.

Ehrenberg, C.G., 1843. Verbreitung und Einfluss des mikroskopischen Lebens in Süd-und Nord Amerika. Königl. Preufs. Akad. Wiss. Berlin 1841 (181).

Farooqui, A., Kumar, A., Swindles, G.T., 2011. Thecamoebian com- munities as proxies of seasonality in Lake Sadatal in the Ganga- Yamuna Plains of North India. Palaeontol. Electron. 15, 3A, 19 pp.

Fishbein, E., Patterson, R.T., 1993. Error weighted maximum likelihood (EWML): a new statistically based method to cluster quantitative micropaleontological data. J. Paleontol. 67, 475–485.

Fluid Imaging Technologies, Inc., 2014. FlowCAM(R) Manual. Version 3.4. Fluid Imaging Technologies, Inc., Scarborough, Maine, USA.

Jyothibabu, R., Arunpandi, N., Karnan, C., Jagadeesan, L., Manojkumar, T.M., Balachandran, K.K., Naqvi, S.W.A., 2018. *Fragilariopsis sp.* Bloom causes yellowish-brown waters off Alappuzha, south-central Kerala coast, India, during the mud bank-upwelling phase. Current Sci. 115 (1), 152–159.

Kitahashi, T., Watanabe, H.K., Tsuchiya, M., Yamamoto, H., Yamamoto, H., 2018. A new method for acquiring images of meiobenthic images using the FlowCAM. MethodsX 5, 1330–1335.

Koenig, I., Mulot, M., Mitchell, E.A.D., 2018. Taxonomic and functional traits responses of Sphagnum peatland testate amoebae to experimentally manipulated water table. Ecol. Indic. 85, 342–351.

Kumar, A., Dalby, P.B., 1998. Identification key for *Holocene lacustrine* arcellacean (thecamoebian) taxa. Palaeontol. Electron. 1 (1), 34.

Lansac-Tôha, F.A., Velho, L.F.M., Costa, D.M., Simões, N.R., Alves, G.M., 2014. Structure of the testate amoebae community in different habitats in a neotropical floodplain. Braz. J. Biol. 74, 181–190.

Liu, B., Booth, R.K., Escobar, J., Wei, Z., Bird, B.W., Pardo, A., Curtis, J.H., Ouyang, J., 2019. Ecology and paleoenvironmental application of testate amoebae in peatlands of the high-elevation Colombian páramo. Quat. Res. 92, 1–19.

Macumber, A.L., Blandenier, Q., Todorov, M., Duckert, C., Lara, E., Lahr, D.J.G., Mitchell, E.A.D., Roe, H.M., 2020. Phylogenetic divergence within the Arcellinida (Amoebozoa) is congruent with test size and metabolism type. Eur. J. Protistol. 72, 125645.

Magonono, M., Oberholster, P.J., Shonhai, A., Makumire, S., Gumbo, J.R., 2018. The presence of toxi and non-toxic cyanobacteria in the sediments of the limpopo river basin: Implications for human health. Toxins 10 (7), 269–292.

Mani, T., Primpke, S., Lorenz, C., Gerdts, G., Burkhardt-Holm, P., 2019. Microplastic pollution in benthic midstream sediments of the Rhine River. Environ. Sci. Technol. 53 (10), 6053–6062.

Marcisz, K., Lamentowicz, M., Galka, M., Colombaroli, D., Adolf, C., Tinner, W., 2019. Response of vegetation and testate amoebae trait composition to fire disturbances in and around a bog in central European lowlands (northern Poland). Quat. Sci. Rev. 208, 129–139.

Mazei, Y., Warren, A., 2012. A survey of the testate amoeba genus Difflugia Leclerc, 1815 based on specimens in the E. Penard and C.G. Ogden collections of the Natural History Museum, London. Part 1: Species with shells that are pointed aborally and/or have aboral protuberances. Protistology 7 (3), 121–171.

Mazei, Y., Warren, A., 2014. A survey of the testate amoeba genus Difflugia Leclerc, 1815 based on specimens in the E. Penard and C.G. Ogden collections of the Natural History Museum, London. Part 2: Species with shells that are pyriform or elongate. Protistology 8 (4), 133–171.

Mazei, Y., Warren, A., 2015. A survey of the testate amoeba genus Difflugia Leclerc, 1815 based on specimens in the E. Penard and C.G. Ogden collections of the Natural History Museum, London. Part 3: Species with shells that are spherical or ovoid. Protistology 9 (1), 3–49.

Medioli, F.S., Scott, D.B., 1983. *Holocene arcellecea* (Thecamoebians) from eastern Canada, 21. Cushman Foundation For Foraminiferal Research special Publication, pp. 5–43.

Medioli, F.S., Scott, D.B., Collins, E.S., McCarthy, F.M.G., 1990a. Fossil thecamoebians: present status and prospects for the future. In: Hemleben, C., Kaminski, M.A., Kuhnt, W., Scott, D.B. (Eds.), In: Paleoecology, Biostratigraphy, Paleoceanography and Taxonomy of Agglutinated Foraminifera. NATOAdvanced Study Institute Series, Series, C., Mathematical and Physical Sciences, vol. 327, pp. 813–840.

Medioli, F.S., Scott, D.B., Collins, E.S., Wall, J.H., 1990b. Thecamoebians from the early Cretaceous deposits of Ruby Creek, Alberta (Canada). In: Hemleben, C., Kaminski, M.A., Kuhnt, W., Scott, D.B. (Eds.), In: Paleoecology, Biostratigraphy, Paleoceanography and Taxonomy of Agglutinated Foraminifera. NATOAdvance d Study Institute Series, Series, C., Mathematical and Physical Sciences, vol. 327, pp. 793–812.

Mulot, M., Marcisz, K., Grandgirard, L., Lara, E., Kosakyan, A., Robroek, B.J.M., Lamentowicz, M., Payne, R.J., Mitchell, E.A.D., 2017. Genetic determinism vs. phenotypic plasticity in protist morphology. J. Eukaryot. Microbiol. 64, 729–739.

Nasser, N.A., Gregory, B.R.B., Steele, R.E., Patterson, R.T., Galloway, J.M., 2019. Behind the organic veil: assessing the impact of chemical deflocculation on organic content reduction and lacustrine Arcellinida (testate amoebae) analysis. Microb. Ecol. http://dx.doi.org/10.1007/s00248-019-01429-0.

Nasser, N.A., Patterson, R.T., Roe, H.M., Galloway, J.M., Falck, H., Palmer, M.J., Spence, C., Sanei, H., Macumber, A.L., Neville, L.A., 2016. *Lacustrine arcellina* (testate amoebae) as bioindicators of arsenic contamination. Microb. Ecol. 72, 130–149.

Neville, L.A., McCarthy, F.M.G., MacKinnon, M.D., 2010. Seasonal environmental and chemical impact on thecamoebian community composition in an Oil Sands reclamation wetland in Northern Alberta. Palaeontol. Electron. 13 (2), 13A, 14 pp.

Patil, J.S., Anil, A.C., 2019. Assessment of phytoplankton photo-physiological status from a tropical monsoonal estuary. Ecol. Indic. 103, 289–300.

Patterson, R.T., Fishbein, A., 1989. Re-examination of the statistical methods used to determine the number of point counts needed for micropaleontological quantitative research. J. Paleontol. 63, 245–248.

Patterson, R.T., Huckerby, G., Kelly, T.J., Swindles, G.T., Nasser, N.A., 2015. Hydroecology of Amazonian lacustrine Arcellinida (testate amoebae): A case study from Lake Quistococha. Peru. Eur, J. Protistol. 51, 460–469.
Patterson, R.T., Kumar, A., 2000a. Assessment of arcellacean (thecamoebian) assemblages, species, and strains as contaminant indicators in James Lake, Northeastern Ontario, Canada. J. Foraminifer. Res. 30, 310–320.
Patterson, R.T., Kumar, A., 2000b. Use of arcellacea to gauge levels of pollution and remediation of industrially polluted lakes. In: Martin, R.E. (Ed.), Environmental Micropaleontology. In: Topics in Geobiology, vol. 15, Kluwer Academic/Plenum Publication, pp. 257–278.
Patterson, R.T., Kumar, A., 2002. A review of current testate rhizopod (thecamoebian) research in Canada. Palaeogeogr. Palaeoclimatol. Palaeoecol. 180, 225–251.
Patterson, R.T., Lamoureux, E.D.R., Neville, L.A., Macumber, A.L., 2013. Arcellacea (Testate Lobose Amoebae) as pH indicators in a pyrite mine-acidified lake, Northeastern Ontario, Canada. Microb. Ecol. 65, 541–554.
Patterson, R.T., Roe, H.M., Swindles, G.T., 2012. Development of an Arcellacea (testate lobose amoebae) based transfer function for sedimentary phosphorous in lakes. Palaeogeogr. Palaeoclimatol. Palaeoecol. 348–349, 32–44.
Penard, E., 1890. Catalog der nackten und schalentragenden Rhizopoden von Weisbaden. Jarbuch der nassavischen Vereins für Naturkunde 43, 67–72.
Penard, E., 1902. Faune Rhizopodique du Bassin du Lèman. Libraire de L'institut, Genéve, p. 712,
Porter, S.A., Knoll, A.H., 2000. Testate amoeba in the Neoproterozoic Era: evidence from vase-shaped microfossils in the chuar group. Grand Canyon. Paleobiology 26, 360–385.
Reinhardt, E.G., Dalby, A.P., Kumar, A., Patterson, R.T., 1998. Arcellaceans as pollution indicators in mine tailing contaminated lake near Cobalt, Ontario, Canada. Micropaleontology 44, 131–148.
Roe, H.M., Patterson, R.T., 2006. Distribution of thecamoebians (testate amoebae) in small lakes and ponds, Barbados, West Indies. J. Foraminifer Res. 36, 116–134.
Roe, H.M., Patterson, R.T., 2014. Arcellacea (testate amoebae) as bio- indicators of road salt contamination in lakes. Microb. Ecol. 68, 299–313.
Roe, H., Patterson, R.T., Swindles, G.T., 2010. Controls on the contemporary distribution of lake thecamoebians (testate amoebae) within the Greater Toronto Area and their potential as water quality indicators. J. Paleolimnol. 43, 955–975.
Sieracki, C.K., Sieracki, M.E., Yentsch, C.S., 1998. An imaging-in-flow system for automated analysis of marine microplankton. Mar. Ecol. Prog. Ser. 168, 285–296.
Steele, R.E., Nasser, N.A., Patterson, R.T., Gregory, B.R.B., Roe, H.M., Reinhardt, E.G., 2018. An assessment of sub-meter scale spatial variability of Arcellinida (testate lobose amoebae) assemblages in a temperate lake: implications for limnological studies. Microb. Ecol. 76 (3), 680–694.
Swindles, G.T., Kelly, T.J., Roucoux, K.H., Lawson, I.T., 2018. Response of testate amoebae to a late Holocene ecosystem shift in an Amazonian peatland. Eur. J. Protistol. 64, 13–19.
Taylor, L.S., Swindles, G.T., Morris, P.J., Galka, M., 2019. Ecology of peatland testate amoebae in the Alaska continuous permafrost zone. Ecol. Indic. 96, 153–162.
Ward, J.H., 1963. Hierarchical grouping to optimize an objective function. J. Amer. Statist. Assoc. 58, 236–244.